



HAL
open science

Semi-automatic Compartment Extraction to Assess 3D Bone Mineral Density and Morphometric Parameters of the Subchondral Bone in the Tibial Knee

Youssef Rabaa, Hamid Bouhadoun, Jean-Denis Laredo, Christine Chappard

► **To cite this version:**

Youssef Rabaa, Hamid Bouhadoun, Jean-Denis Laredo, Christine Chappard. Semi-automatic Compartment Extraction to Assess 3D Bone Mineral Density and Morphometric Parameters of the Subchondral Bone in the Tibial Knee. 19th International Conference on Information Visualisation (iV), Jul 2015, Barcelone, Spain. pp.518-523, 10.1109/iV.2015.92 . hal-01436797

HAL Id: hal-01436797

<https://hal.science/hal-01436797v1>

Submitted on 10 Sep 2024

HAL is a multi-disciplinary open access archive for the deposit and dissemination of scientific research documents, whether they are published or not. The documents may come from teaching and research institutions in France or abroad, or from public or private research centers.

L'archive ouverte pluridisciplinaire **HAL**, est destinée au dépôt et à la diffusion de documents scientifiques de niveau recherche, publiés ou non, émanant des établissements d'enseignement et de recherche français ou étrangers, des laboratoires publics ou privés.

Semi-automatic compartment extraction to assess 3D bone mineral density and morphometric parameters of the subchondral bone in the tibial knee

Rabaa Youssef*, Hamid Bouhadoun†, Jean Denis Laredo‡, Christine Chappard†

*CEA LinkLab in TELNET INNOVATION LABS, Ariana, Tunisia

rabaa.youssef@supcom.tn

†B2OA Laboratory, UMR CNRS 7052

Université Paris Diderot, PRES Sorbonne Paris Cité, Paris, France

hamid.bouhadoun@paris7.jussieu.fr, christine.chappard@inserm.fr

‡Service de Radiologie Ostéo-Articulaire

Hôpital Lariboisière, Paris, France

jean-denis.laredo@lrb.ap.hp.fr

Abstract—We present a new semi-automatic method to extract the bone mineral density (BMD) and bone proportion (BV/TV) with the aim to analyze subchondral bone changes due to knee osteoarthritis in clinically relevant compartments (medial versus lateral) and (anterior versus posterior). This method based on convex hull is developed initially on high resolution peripheral computed tomography but can potentially be applied in clinical CT with sufficient resolution.

Index Terms—HR-pQCT; subchondral bone; tibia; convex hull; region of interest; BMD; BV/TV

I. INTRODUCTION

Osteoarthritis is a joint disorder that causes pain, stiffness and decreased mobility. The main treatment is to control pain, to reduce stiffness and ultimately the joint replacement is necessary. Knee osteoarthritis OA presents the greatest morbidity and commonly affects the medial compartment [1]. OA is characterized by cartilage loss, abnormal subchondral bone with an increase of bone mineral density (BMD) due to osteosclerosis. Usually osteosclerosis is assessed on radiographs based on the Kellgren Lawrence scoring [2] and few authors have proposed to assess the variation of BMD by Dual X-ray Absorptiometry [3]. It was also possible to assess the microarchitecture changes of the subchondral bone by MRI at 7 Teslas [4]. Locally, the bone proportion or Bone Volume/Total Volume (BV/TV,%) has been shown to be increased in advanced OA from micro-computed tomography images comparatively to normal bone [5]. Subregional changes of volumetric BMD beneath lateral and medial compartments have been already investigated with computed tomography and differences have been noted between normal and mild OA knees [6]. High resolution peripheral computed tomography (HR-pQCT) are usually used at the tibia and the radius for assessing separately the trabecular and cortical bone BMD and the trabecular bone micro-architecture especially

it allows BV/TV estimation which is decreased in case of osteoporosis [7].

New dedicated systems based on cone beam computed tomography, which provide enough image quality and with favorable dose characteristics, are under development [8] [9]. With these new systems, it would be able to follow subchondral bone changes induced by OA in 3D.

Based on 3D image of the knee, it would be interesting to study the microstructure of the subchondral bone in normal and OA knees. In the future, in longitudinal studies, it will allow to better identify early stage of subchondral bone changes, to improve the understanding of the role of this tissue in knee OA and to assist the development of targeted treatment.

The aim of the study is to develop a semi-automatic method of segmentation of the subchondral bone in the tibial compartments of the knee to assess 3D local variation of BMD and BV/TV from HR-pQCT images. For this purpose, we standardize bone regions of interest (ROIs) extraction by constructing convex hulls of the bone surface and partitioning the volume in different compartments. The convex hull method has been used for the neuro-retinal optic cup boundary estimation. It improves the accuracy of the neuro-retinal cup-to-disc ratio measurement which is efficient to diagnose glaucoma [10]. Convex hull is a geometric representation and was used for skeletal bone age evaluation on x-rays of hands [11]. It was also used to automate the global spatial normalization of human brain [12]. In this work, we perform a segmentation of the bone followed by the determination of the closest parallelepiped to the bone surface using a union convex hull. Based on the bone volume obtained, we partition it in compartments and measure BMD

and BV/TV.

The work is organized in two sections. The first section is dedicated to the description of the materials and image processing methods used to conceive the semi-automatic ROIs extraction procedure. In the second section, the stability of the extraction procedure is evaluated, the results of BV/TV on normal tibial knees are presented according to the different compartments with a final discussion.

II. MATERIALS AND METHODS

Ten knee specimens (5 women, 5 men; mean age: 79.0 ± 13.0 years) were collected at the Institute of Anatomy Paris Descartes. Collection of these human tissue specimens was conducted according to pertinent protocols established by the Human Ethics Committee at Inserm. Due to this regulation, no data were available regarding the cause of death, previous illnesses, or medical treatments of these individuals. Soft tissues were removed from the tibias which were stored at -20°C . X-rays are performed to define the Kellgren Lawrence (KL) scoring [2], the 10 selected knees have a KL score > 2 and consequently are considered as normal.

Scans by HR-pQCT (Xtrem CT Scanco Medical Brüttisellen, Switzerland) were performed to obtain volumetric BMD of the trabecular bone: D_{trab} , in mg hydroxyapatite/cm³ and the derived parameter the bone proportion (BV/TV, %) according to the manufacturer procedure. Shortly, HR-pQCT scans provided high resolution images with a nominal isotropic voxel size of 82 microns and attenuation data were converted to equivalent hydroxyapatite (HA) densities. The BV/TV measurements were derived from D_{trab} (i.e. $BV/TV(\%) = 100 * (D_{\text{trab}}(\text{mgHA}/\text{cm}^3)/1200\text{mgHA}/\text{cm}^3)$). To obtain images of the knees, 660 to 880 slices were necessary for each scan. Only the tibial part was analyzed in our study. Therefore, the volume of interest of the studied subchondral bone is selected in the tibial plateau under the cortical plate. The first slice corresponds to the top of the fibulae. The volume of interest needs to be specified for each knee, because of their varying size. The number of slices analyzed per knee is between 103 to 180 (mean 146).

In a first subsection, we describe the segmentation of bone on each slice. Second, we present the automatic construction of the parallelepiped circumscribed to bone volume. Finally, we partition the surface in medial/lateral and anterior/posterior compartments.

A. Semi-automatic bone extraction

This procedure should be able to manage the variable size, geometry and positioning of the tibial bone in the sequence of images in order to obtain the closest rectangle to the bone throughout the volume selected by the operator. In fact, once the segmentation is done, we calculate the union of

convex hulls of the bone surface throughout the slices from which we deduce the circumscribed rectangle. Consequently, we construct the closest straight parallelepiped containing the entire bone volume with standardized ROIs. In order to estimate precisely the position of the convex hull at each slice, we need to proceed a segmentation that separates the bone from the soft tissue.

First, we show in Figure 1 the gray levels histogram of a DICOM image. We indicate on the figure the background, soft tissue and bone gray levels range and notice that bone has no specific mode on the histogram, compared to soft tissue. We deduce that for these images, classical thresholding methods fail.

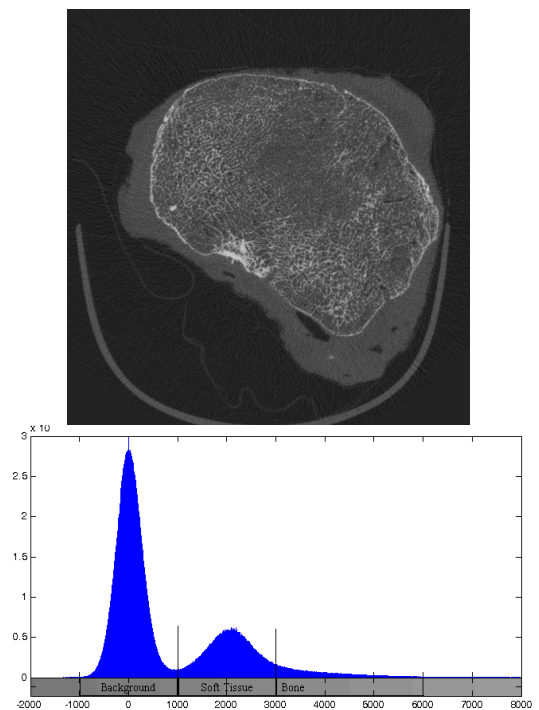


Fig. 1. Example of DICOM histogram of one slice

Our aim is to detect the entire cortical bone to correctly construct the convex hull. However, a direct thresholding fails when there are holes in the cortical bone, when the knee is deformed by OA or when mean gray levels of the soft tissue are close to bone one as it is shown in Figure 1. Therefore, we perform image preprocessing operations using an average filter (convolution with a disk structuring element of 9 pixels size) to smooth both soft tissue and bone.

$$I' = I * H$$

I is the original DICOM image, H is the structuring element and I' the averaged image. The smoothing permits to find a stable quantile (q) of the gray levels separating bone from soft tissue. This quantile is used as a threshold level to binarize the treated slices. However, its value cannot be set similarly for all knees and needs to be set by the operator according to

the following recommendations. In fact, through observations, we notice that this quantile is in the range $[0.75, 0.9]$ since the bone gray values are in the upper bound of the volume histogram (see Figure 1).

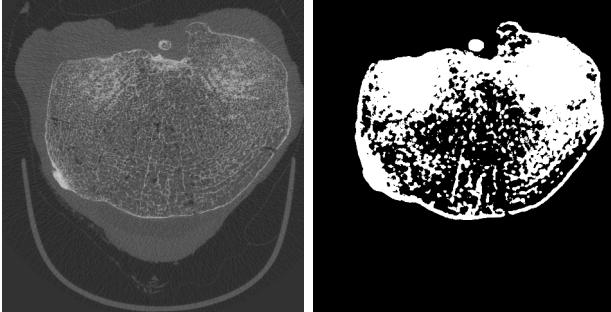


Fig. 2. Left: DICOM image. Right: binary mask

This quantile varies depending on of the size of the knee and the quality of its trabecular and cortical bone. The smoothing permits to eliminate residuals in the soft tissue and to enhance cortical bone contour (see Figure 2).

After segmentation step, we use in addition morphological closing and opening operations to fill holes of the bone region and to eliminate residuals (if any) in order to obtain a mask that covers the entire bone surface. This mask is obtained as follows:

$$\text{Bone Mask} = (\text{Binary slice} \bullet D) \circ D$$

where \bullet is the closing operation and \circ is the opening one. Both operations use disk structuring element D of radius 30.

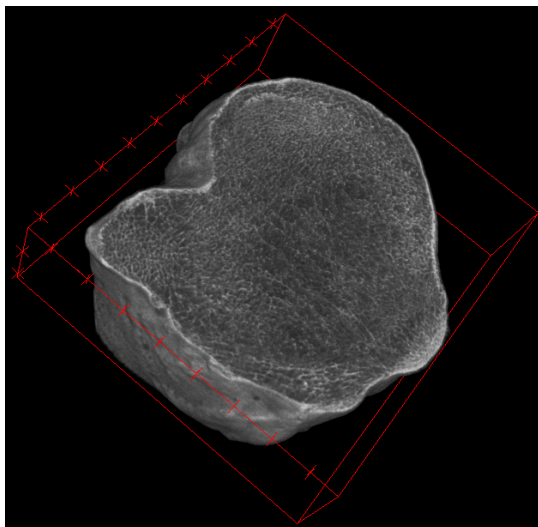


Fig. 3. Bone volume without soft tissue surrounding. In red the hypothetical circumscribed parallelepiped.

Once the masks of the slices are created, we apply them on the original images to obtain an extracted bone volume as presented in Figure 3.

B. Automatic convex hull construction and partitioning in ROIs

After the segmentation step, we use the convex hull of each segmented bone to calculate the union of the convex hulls. From this union convex hull, we determine the direction of the major axis of the ellipse having the same second moments as the envelope, and then calculate the rectangle vertices. Figure 4 illustrates the described steps. One can observe from Figure 4.(c) the varying size of tibial bone since the obtained union convex hull does not fit to the cortical envelope for all slices.

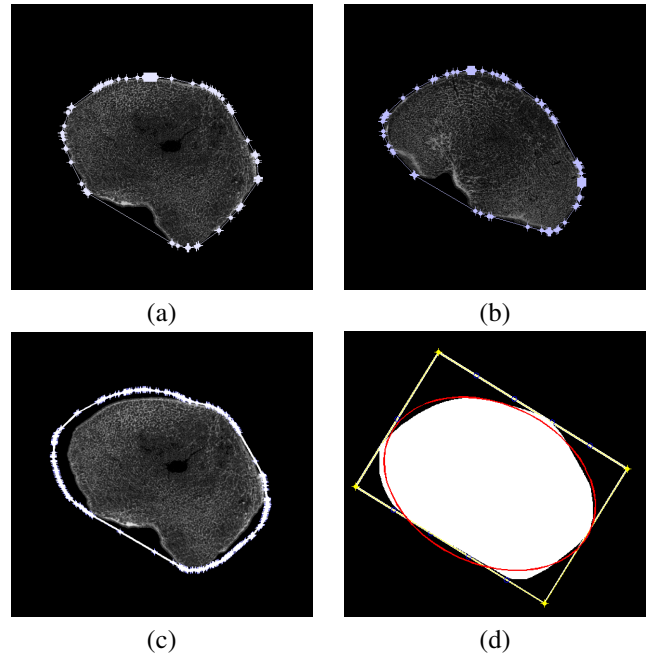


Fig. 4. (a) and (b): First and last slices of the tibial volume with respective convex hulls. (c): Union of all volume convex hulls superimposed on first slice. (d): In yellow, circumscribed rectangle and in blue, the calculated positions of ROIs summits on the rectangle.

After detecting the bone envelope and constructing the circumscribed rectangle, we define the partitioning of the slices in regions of interest. Based on this partitioning, we measure BMD and bone proportion on each compartment and analyse possible variations. On each slice, we propose to consider 4 different regions of interest (ROIs) clinically relevant. We separate medial compartment from lateral one and also posterior area from the anterior one with the aim to make comparison of the BV/TV in between the 4 regions. The 4 ROIs circumscribed into the bone are shown in Figure 5.

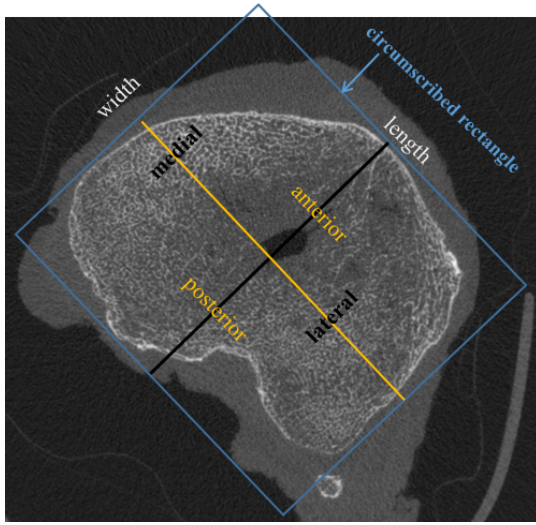


Fig. 5. Description of the knee anatomy and the position of the circumscribed rectangle

The central zone that corresponds to the tibial spine area between medial and lateral compounds is removed from the analysis since it does not provide any relevant information. The bone surface partitioning in compartments on each slice is set after acquiring the position of the circumscribed rectangle. This final step of bone partitioning is illustrated on Figure 6 with labeled ROIs of a slice.

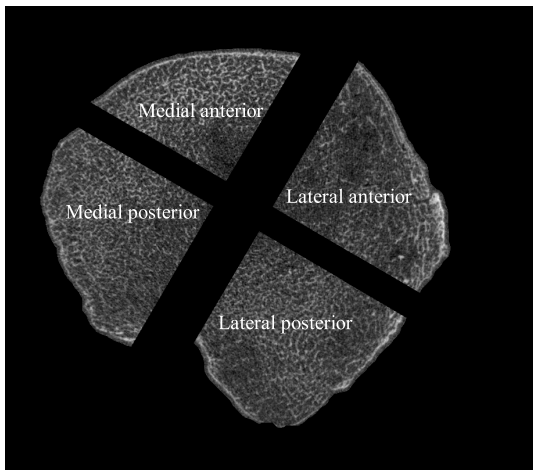


Fig. 6. Slice partitioned in ROIs with respective labels

The block diagram of Figure 7 summarizes the main steps of the proposed extraction. The segmentation step is semi-automatic since it depends on the quantile parameter q_{level} which is linked to the amount of bone in the knee. The union convex hull construction followed by the circumscribed rectangle definition and partitioning in ROIs is automatic and user-independent. The automation of this step enables the user to standardize ROIs extraction and perform further analysis of the bone per region.

III. RESULTS AND DISCUSSION

In this section, we present results of the semi-automatic extraction of ROIs. First, we evaluate the user-dependency of the proposed procedure using a reproducibility test. We also test the effect of thresholding changes on the results. Then, we calculate variation of BV/TV using mean gray values on ROIs and discuss the results.

A. Reproducibility and Deviation Tests

For the first test, the Root Mean Square Coefficient Variation RMSCV was used [13]. Two users performed the ROIs extraction of 10 knees and adjusted the quantiles using the recommendations cited in this work and by checking visually the bone surface segmentation. The Root Mean Square Coefficient of Variation was calculated on the mean gray values found by each user on a knee slices. The RMSCV following formula was used:

$$RMSCV(\%) = \frac{\sqrt{\sum_{k=1}^n d_i^2 / 2 \cdot n}}{(m_1 + m_2) / 2} * 100$$

where n is the size of the sample (10 knees), d_i is the deviation between the 2 users mean gray values on a knee, m_1 is the mean gray value on the knees for User1 (skilled) and m_2 is the mean gray value of the knees for User2 (unskilled). The RMSCV was calculated on each ROI. Table 1 resumes the results.

TABLE I
REPRODUCIBILITY TEST ON ROIs.

Knee compartments	Medial anterior	Lateral anterior	Medial posterior	Lateral posterior
RMSCV%	0.64	0.41	2.03	2.78

For the second test, the deviation from the reference was estimated with ± 0.02 quantile variations. We used the Root Mean Square Standard Error (RMSSE, %) with the following formula:

$$RMSSE(\%) = \frac{\sqrt{\sum_{k=1}^n d_i^2 / n}}{1/n \cdot \sum_{k=1}^n V_{ref}} * 100$$

where V_{ref} refers to the mean gray values of the reference knee, n the number of knees (10) and d_i the deviation between the reference and the new value after quantile variation.

TABLE II
DEVIATION ERROR WITH QUANTILE VARIATION ± 0.02 .

Knee compartments	Medial anterior	Lateral anterior	Medial posterior	Lateral posterior
RMSSE% +0.02	12.87	11.38	18.40	8.35
RMSSE% -0.02	6.52	12.34	9.09	5.56

B. Morphometric parameters of bone compartments

For each compartment, 103 to 180 slices were analyzed according to the size of the knee and divided in 3 vertical segments corresponding approximately to 0 to 4mm, 4mm to

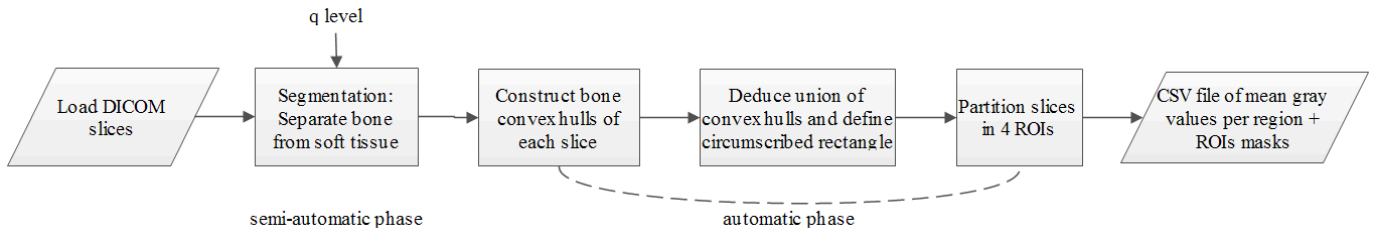


Fig. 7. Semi-automatic compartment extraction of subchondral bone in the tibial knee.

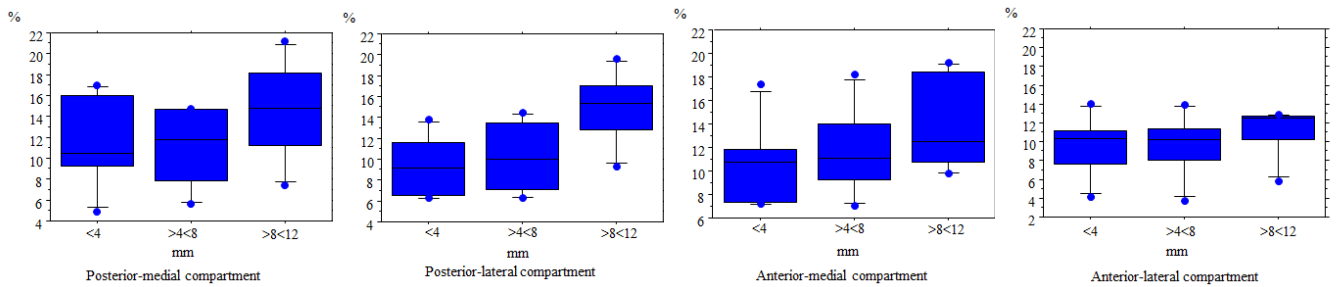


Fig. 8. The BV/TV, % results on each compartments divided in 3 vertical segments from the articular surface.

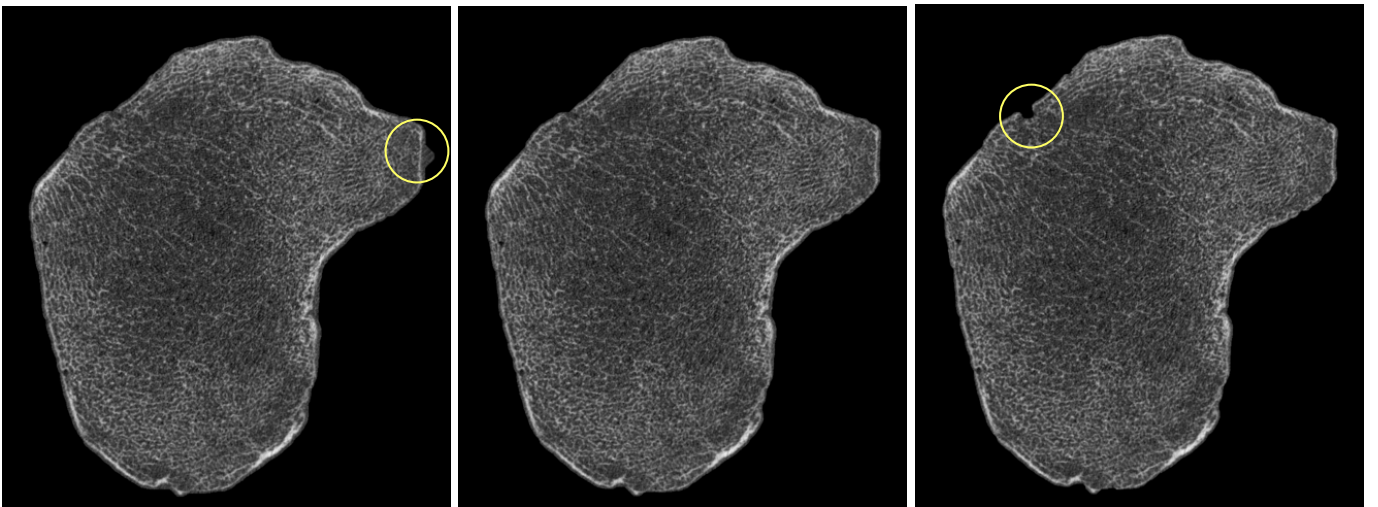


Fig. 9. Thresholding variation easily supervised and checked by user. Left: $q = 0.89$ (soft tissue surrounding bone). Center: $q = 0.87$ (right threshold). Right: $q = 0.85$ (bone defect).

8 mm and 8mm to 12 mm starting from the tibial surface to the depth of the tibial metaphysis. The BV/TV results were shown in the Figure 8. There is a tendency of higher BV/TV in the posterior medial compartment comparatively to the others. In all compartments, the mean BV/TV increase after 8 mm deep. The BMD data are not shown because they are paralleled to BV/TV data which are directly derived from the BMD ones.

C. Discussion

We describe here a reliable method for subchondral bone extraction in HR-pQCT images to measure BMD and BV/TV. According to the block diagram of Figure 7, one can deduce that the pertinence of the extraction depends on the chosen

quantile for the threshold of the volume before the construction of the bone mask. This quantile is fixed depending on the amount of bone for a knee. For example, a knee where the BMD is low, the quantile is about $q_{level} = 0.87$. On the contrary, a knee where the BMD is high the quantile is about $q_{level} = 0.8$. The accuracy of the thresholding step can be easily checked by the user. Indeed, the reproducibility between a skilled and unskilled user is low under 3%. In other respect, we have tested ± 0.02 changes of the threshold value, either soft tissue appeared or bone disappeared in a non-realistic manner as illustrated by Figure 9.

IV. CONCLUSION

We describe here a reliable method for subchondral bone extraction in HR-pQCT images to measure BMD and BV/TV in different compartments. We found BV/TV discrepancies between the different compartments and depending on the depth position. It would be interesting to compare with OA knees, this could help to a better understanding of OA process in different compartments.

ACKNOWLEDGEMENTS

ANR Voxelo TECS-0018.

REFERENCES

- [1] T. Neogi and Y. Zhang, "Epidemiology of osteoarthritis," *Rheumatic Disease Clinics of North America*, vol. 39, no. 1, pp. 1 – 19, 2013, update on Osteoarthritis. [Online]. Available: <http://www.sciencedirect.com/science/article/pii/S0889857X12001160>
- [2] J. H. Kelleghren and J. S. Lawrence, "Radiological assessment of osteoarthritis," *Annals of Rheumatic Diseases*, vol. 16, no. 4, pp. 494–502, 1957.
- [3] O. Bruyere, C. Dardenne, E. Lejeune, B. Zegels, A. Pahaut, F. Richey, L. Seidel, O. Ethgen, Y. Henrotin, and J. Y. Reginster, "Subchondral tibial bone mineral density predicts future joint space narrowing at the medial femoro-tibial compartment in patients with knee osteoarthritis," *Bone*, vol. 32, no. 5, pp. 541–5, 2003.
- [4] G. Chang, H. Stephen, L. Yinxiang, C. Cheng, C. Kevin, R. Chamith, E. Kenneth, X. Ding, S. Punam, and R. Ravinder, "7tesla mri of bone microarchitecture discriminates between women without and with fragility fractures who do not differ by bone mineral density," *Journal of Bone and Mineral Metabolism*, pp. 1–9, 2014. [Online]. Available: <http://dx.doi.org/10.1007/s00774-014-0588-4>
- [5] C. Chappard, F. Peyrin, A. Bonnassie, G. Lemineur, B. Brunet-Imbault, E. Lespessailles, and C.-L. Benhamou, "Subchondral bone micro-architectural alterations in osteoarthritis: a synchrotron micro-computed tomography study," *Osteoarthritis and Cartilage*, vol. 14, no. 3, pp. 215 – 223, 2006. [Online]. Available: <http://www.sciencedirect.com/science/article/pii/S1063458405002645>
- [6] K. L. Bennell, M. W. Creaby, T. V. Wrigley, and D. J. Hunter, "Tibial subchondral trabecular volumetric bone density in medial knee joint osteoarthritis using peripheral quantitative computed tomography technology," *Arthritis & Rheumatism*, vol. 58, no. 9, pp. 2776–2785, 2008. [Online]. Available: <http://dx.doi.org/10.1002/art.23795>
- [7] S. Boutroy, M. L. Bouxsein, M. Munoz, and P. D. Delmas, "In vivo assessment of trabecular bone microarchitecture by high-resolution peripheral quantitative computed tomography," *The Journal of Clinical Endocrinology & Metabolism*, vol. 90, no. 12, pp. 6508–6515, 2005.
- [8] W. Zbijewski, P. D. Jean, P. Prakash, Y. Ding, J. W. Stayman, N. Packard, R. Senn, D. Yang, J. Yorkston, A. Machado, J. A. Carrino, and J. H. Siewerdsen, "A dedicated cone-beam ct system for musculoskeletal extremities imaging: design, optimization, and initial performance characterization," *Medical Physics*, vol. 38, no. 8, pp. 4700–13, 2011.
- [9] J. A. Carrino, A. A. Muhiit, W. Zbijewski, G. K. Thawait, J. W. Stayman, N. Packard, R. Senn, D. Yang, D. H. Foos, J. Yorkston, and J. H. Siewerdsen, "Dedicated cone-beam ct system for extremity imaging," *Radiology*, vol. 270, no. 3, pp. 816–824, 2014.
- [10] Z. Zhang, J. Liu, N. S. Cherian, Y. Sun, J. H. Lim, W. K. Wong, N. M. Tan, S. Lu, H. Li, and T. Y. Wong, "Convex hull based neuro-retinal optic cup ellipse optimization in glaucoma diagnosis," in *Engineering in Medicine and Biology Society, 2009. EMBS 2009. Annual International Conference of the IEEE*, Sept 2009, pp. 1441–1444.
- [11] D. Giordano, R. Leonardi, F. Maiorana, G. Scarciofalo, and C. Spampinato, "Epiphysis and metaphysis extraction and classification by adaptive thresholding and dog filtering for automated skeletal bone age analysis," in *Engineering in Medicine and Biology Society, 2007. EMBS 2007. 29th Annual International Conference of the IEEE*, Aug 2007, pp. 6551–6556.
- [12] J. L. Lancaster, P. T. Fox, H. Downs, D. S. Nickerson, T. A. Hander, M. E. Mallah, P. V. Kochunov, and F. Zamarripa, "Global spatial normalization of human brain using convex hulls," *Journal of Nuclear Medicine*, vol. 40, no. 6, pp. 942–55, 1999.
- [13] C. C. Glüer, G. Blake, Y. Lu, B. A. Blunt, M. Jergas, and H. K. Genant, "Accurate assessment of precision errors: How to measure the reproducibility of bone densitometry techniques," *Osteoporosis International*, vol. 5, no. 4, pp. 262–270, 1995. [Online]. Available: <http://dx.doi.org/10.1007/BF01774016>